Journal of Medicinal Chemistry

Article

Virtual Screening of Novel CB2 Ligands Using a Comparative Model of the Human Cannabinoid CB2 Receptor

Outi M. H. Salo, Katri H. Raitio, Juha R. Savinainen, Tapio Nevalainen, Maija Lahtela-Kakkonen, Jarmo T. Laitinen, Tomi Jrvinen, and Antti Poso

J. Med. Chem., **2005**, 48 (23), 7166-7171• DOI: 10.1021/jm050565b • Publication Date (Web): 18 October 2005

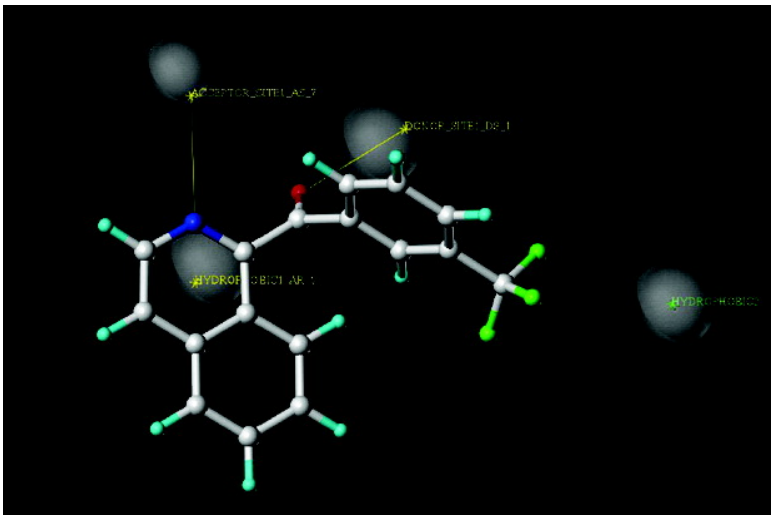

More About This Article

Additional resources and features associated with this article are available within the HTML version:

- Supporting Information
- Links to the 6 articles that cite this article, as of the time of this article download
- Access to high resolution figures
- Links to articles and content related to this article
- Copyright permission to reproduce figures and/or text from this article

View the Full Text HTML

Journal of Medicinal Chemistry is published by the American Chemical Society. 1155 Sixteenth Street N.W., Washington, DC 20036

Virtual Screening of Novel CB2 Ligands Using a Comparative Model of the Human Cannabinoid CB2 Receptor

Outi M. H. Salo,*,† Katri H. Raitio,† Juha R. Savinainen,‡ Tapio Nevalainen,† Maija Lahtela-Kakkonen,† Jarmo T. Laitinen,‡ Tomi Järvinen,† and Antti Poso†

Department of Pharmaceutical Chemistry and Department of Physiology, University of Kuopio, P.O. Box 1627, FIN-70211 Kuopio, Finland

Received June 16, 2005

To identify novel selective CB2 lead compounds, a comparative model of the CB2 receptor was constructed using the high-resolution bovine rhodopsin X-ray structure as a template. The CB2 model was utilized both in building the database queries and in filtering the hit compounds by a docking and scoring method. In G-protein activation assays, 1-isoquinolyl[3-(trifluoromethyl)phenyl]methanone (**40**, NRB 04079) was found to act as a selective agonist at the human CB2 receptor.

Introduction

The cannabinoid CB2 receptor is a G-protein-coupled receptor (GPCR) located mainly in immune tissues.[1,2] It is part of the endogenous cannabinoid system (ECS) that includes the endocannabinoids (e.g., 2-arachidonoylglycerol [2-AG]), their receptors (CB1 and CB2), metabolizing enzymes (fatty-acid amide hydrolase [FAAH] and monoglyceride lipase [MGL]), and a specific cellular uptake system.[3−6] The ECS is an attractive target for drug development, and various cannabinergic ligands that act on one or more ECS target proteins have been developed during recent years.[3,7] The CB2 receptor ligands possess potential in alleviating pain[8] and inflammation,[9] as well as in treatment of chronic cough,[10] gliomas,[11] lymphomas,[12] and osteoporosis.[13] Many cannabinoid receptor ligands are nonselective in that they bind both to the central CB1 receptor as well as the peripheral CB2 receptor. It is claimed that selective CB2 ligands should be devoid of the unwanted central nervous system (CNS) effects typical of Δ^9-tetrahydrocannabinol (Δ^9-THC), the major psychoactive component of *Cannabis sativa* L.[14] Many of the CB2 selective agonists currently under study are based on the classical cannabinoid structure (e.g., **14**, JWH-133[15] and **17**, HU-308[16]) or cannabimimetic indoles (e.g., **26**, AM1241[17] and **27**, GW405833[18]), whereas the CB2 antagonists or inverse agonists can have, for example, a pyrazole- or an oxoquinoline-based scaffold (**20**, SR144528[19] and **28**, JTE−907,[9] respectively). See Supporting Information (Section A) for the chemical structures of these and other CB2 ligands utilized in our study.

In the present study, we have employed a structure-based virtual screening procedure to search for novel CB2 selective lead compounds with alternative molecular scaffolds. In the absence of an experimental structure of the individual GPCRs, rhodopsin crystal structure[20]-based comparative models have been shown to be useful for structure-based virtual screening and lead optimization.[21−23] Recently, Xie et al.[24] and Montero et al.[25] have generated rhodopsin-based comparative models of CB2, but neither study employed the models in virtual screening. In this study, the constructed comparative model of the CB2 receptor was utilized both in building the database queries as well as in filtering the hit molecules by docking and scoring.

Results and Discussion

Comparative Model of CB2. In the present study, the comparative model of CB2 was constructed in a similar fashion as previously described for the CB1 receptor.[26] In addition to ignoring the coordinates of the highly conserved proline P5.50(215) at the rhodopsin template, also the coordinates of G2.56(89) were omitted from the CB2 model without extensively disturbing the α-helical structure (Figure 1A). Due to the latter deletion, the TM2 (transmembrane helix 2) kink introduced by the GG motive in rhodopsin was straightened at CB2, and F2.57(87) of CB2 was aligned with F2.58(91) of rhodopsin thus becoming a part of the putative binding site. Furthermore, C2.59(89) of CB2 that has been suggested to reside at the margin of the binding site[27] was now located in the TM2-3 interface instead of facing out to lipid as the corresponding residue in rhodopsin (see Supporting Information, Sections B and C). The molecular dynamics simulation for the refinement of the CB2 model gave comparable results with the CB1 model (see Supporting Information, Sections D−F). The final structure from the MD simulation (model 1) and four other CB2 receptor conformers created by the simulated annealing procedure (models 2−5) were compared with each other by generating crude CoMFA models for the CB2 ligands docked at these receptor conformers (see Supporting Information, Sections G and H for detailed ligand−receptor interactions and figures of docking alignments). Due to the differences between the affinity measurements of different laboratories, the biological data used in the CoMFA models was not consistent. Also, for some racemic molecules we did not know which enantiomer (*R* or *S*) was the active form, and therefore we used both of them in our assessment. Consequently,

* To whom correspondence should be addressed. Tel: +358-17-163714. Fax: +358-17-162456. E-mail: outi.salo@uku.fi.
† Department of Pharmaceutical Chemistry.
‡ Department of Physiology.

10.1021/jm050565b CCC: $30.25
Published on Web 10/18/2005

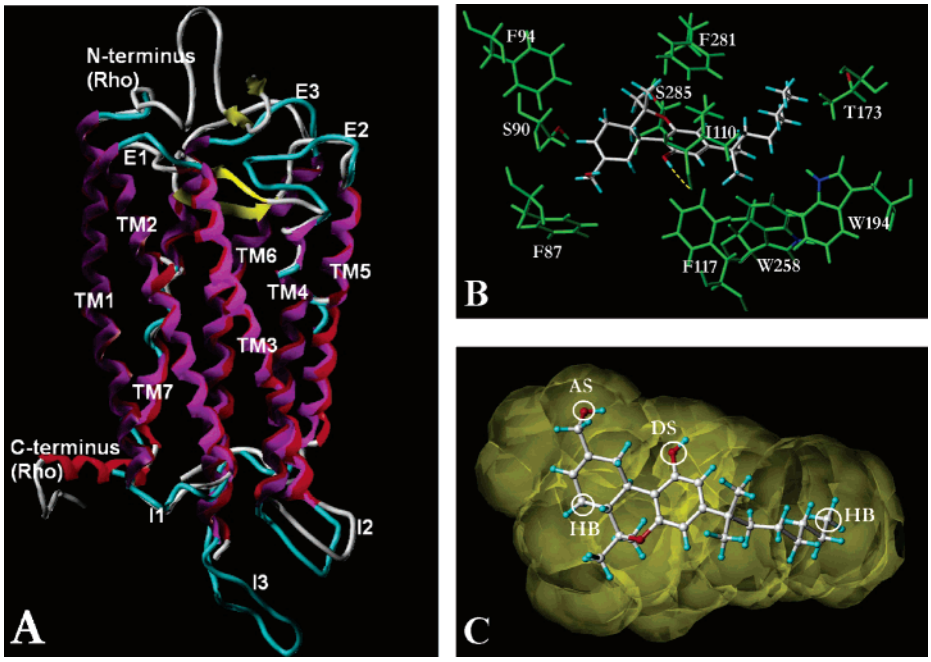

Figure 1. (A) CB2 model compared with the rhodopsin crystal structure (Rho). Secondary structure coding; α-helix − purple (CB2)/red (Rho), β-sheet − yellow, other − cyan (CB2)/white (Rho). (B) Docking orientation of **7** at the CB2 receptor model. H-bond between the phenolic hydroxyl of **7** and the backbone oxygen of I3.29(110) is indicated with a yellow dashed line. Atom color code: green, protein backbone and side chain carbon/hydrogen atoms; blue, nitrogen; red, oxygen; gray, carbon; cyan, hydrogen. (C) Molecular graphics of query 1; pharmacophoric query features were based on the docked conformation of **7**; AS − acceptor site; DS − donor site; HB − hydrophobic feature. Multiple volume surface of six docked CB2 ligands was used as a volume constraint (yellow).

the CoMFA models in general were neither excellently robust nor predictive. Receptor model 1, however, resulted in the best cross-validation and progressive scrambling values (Supporting Information, Sections I and J) and thus was chosen to be utilized in the database screening.

Although our main aim was not to create an exact docking model for the CB2 ligands, examining molecular interactions of representative compounds at receptor model 1 let us suggest that hydrophobic contacts and aromatic stacking interactions, rather than hydrogen bonding, are of great importance at the putative CB2 binding site. Several groups have studied the importance of different receptor residues for the ligand binding or signal transduction at CB2. The present model is in agreement with the results of Tao et al.[28] who reported that K3.28(109) in CB2 is not important for ligand binding, contrary to the corresponding lysine in CB1. In our model, the studied compounds did not have any H-bonds with this residue. Furthermore, S7.39(285) that has been suggested to be a site of interaction for the cannabinoid agonist HU-243[29] is part of the putative binding pocket in the present model. Among the aromatic microdomain residues[30] (F3.25, F3.36, W4.64, Y5.39, F5.43, W6.48), W4.64(172), and Y5.39(190) have been shown to be critical for ligand binding.[31,32] However, instead of being in direct interaction with the ligands, it has been suggested that these residues are important for the arrangement of the other aromatic residues in the receptor binding pocket. This is in agreement with our docking model as in most of the cases there are no direct stacking interactions with these aromatic residues (Supporting Information, Section G).

It is worth mentioning that similarly with our CB1 model, the side chain chi1 rotamer of W6.48(258) changed from gauche+ to trans during the MD simulation (see ref 26). This rotamer change has been suggested to be a "toggle switch" for the CB1 receptor activation.[33,34] In addition to the conformational changes of single amino acid side chains, it is evident that the GPCR activation is accompanied by rigid domain motions and rotations of TM helices. However, we did not apply such rotations on our model. Due to the conformational changes during the MD simulation, the present model may, nonetheless, represent an intermediate state (neither active, nor inactive) of the receptor even though the original rhodopsin template used for the comparative modeling was in its inactive state.

Database Searches. Both the docked CB2 ligand structures and the model 1 receptor binding site were employed in building the three-dimensional (3D) database queries. Query 1 (Q1) was based on the pharmacophoric points of the nonselective cannabinoid receptor agonist **7** (HU-210) and the multiple volume surface of six CB2 agonists (**7**, **11** [L759633], **12** [L759656], **16** [CP55940], **17**, **26**), all in their docking conformations (Figures 1B and 1C). The second query (Q2) was based on the binding cavity of the docked CB2 ligands, whereas the third query (Q3) was based on the combination of features taken from both the receptor and bound ligands. The overall screening and filtering process is presented in Figure 2. Finally, 86 hit molecules (0.15% of the whole database) were ordered from Maybridge to be tested for their in vitro activity at the CB2 receptor.

Biological Evaluation of the Hits. All hit molecules were screened for their G-protein activation of the human CB2 receptor. The preliminary screening in cell lysates identified a compound that stimulated

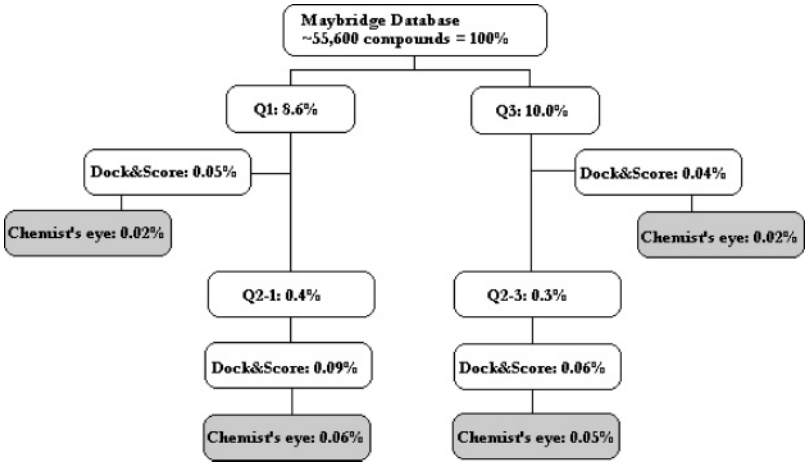

Figure 2. Overview of the database screening procedure. The percentages represent the number of compounds from the Maybridge database. Q1 = hits found with query 1; Q3 = hits found with query 3; Q2−1 = hits found with query 2 from the results of Q1; Q2−3 = hits found with query 2 from the results of Q3.

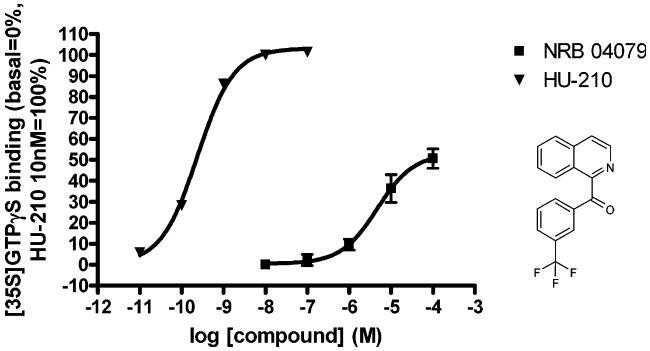

Figure 3. The dose−response curves for the CB2 receptor agonists **7** and **40**. The data are expressed as mean ± SEM of at least three independent experiments performed in duplicate. Chemical structure of **40** is shown next to its curve.

G-protein activity, while a few others inhibited G-protein activation (data not shown). Further characterization in CHO-hCB2 cell (and control CHO cell) membranes confirmed that **40** (NRB 04079) (Figure 3) behaves as a true CB2 agonist, whereas the compounds with inhibitory effects were found not to act via CB2. A more detailed dose−response study revealed that **40** is a low-potency partial agonist at the CB2 receptor ($-\log EC_{50} = 5.3 \pm 0.2$; $E_{max} = 53 \pm 4$ %) when compared with the potent full agonist **7** ($-\log EC_{50} = 9.6 \pm 0.0$; $E_{max} = 103 \pm 1$%; Figure 3). Compound **40**, therefore, can serve as a lead structure for designing selective CB2 agonists that are useful, for example, in the management of pain. Compound **40** was found with query 1, and it is rather suitable for lead optimization, as it is relatively small and has a definite scaffold to modify. According to the docking results, aromatic stacking interactions, rather than hydrogen bonding, seem to be important also for this ligand at the CB2 receptor (see Supporting Information, Section G for detailed description of ligand−receptor interactions).

Since the cannabinergic compounds usually act unselectively on one or more target proteins of the ECS, the lead compound was tested also for the G-protein activation at the CB1 receptor as well as for the inhibition of the FAAH and MGL enzymes (for MGL assay method, see ref 35; FAAH assay, unpublished results of Saario et al.; data not shown). Confirming its CB2 selectivity, **40** did not possess any CB1 activity, nor did it inhibit either of the enzymes.

Conclusions

The present study demonstrates that combined ligand- and structure-based virtual screening is a useful tool for detecting novel lead compounds for the GPCRs such as the CB2 receptor. Here, we describe the discovery of a selective CB2 agonist with the help of a comparative model for the CB2 receptor. In particular, the docking of known CB2 ligands at the receptor binding site played an important role in the virtual screening process. The hit molecule serves as a lead structure for novel CB2 agonists that are intended for therapeutic use.

Experimental Section

Computational Methods. HOMOLOGY module of InsightII v.2000[36] modeling software was utilized to construct the CB2 receptor model, whereas structure optimization, visualization, and ligand structure construction were carried out using the SYBYL 6.9[37] modeling package. Molecular dynamics (MD) simulations were performed with GROMACS v.3.1.4,[38,39] and the stereochemical quality of the protein structures was checked with PROCHECK.[40] GOLD 2.0[41] was used for ligand docking, and both CScore[42] and X-Score v1.1[43,44] for ranking the docking results. CoMFA,[45] as implemented in SYBYL, was used for generating 3D-QSAR models. Lead structure searches in the Maybridge[46] molecular database were carried out with UNITY 4.4[47] module of SYBYL. Default options were used in the programs if not otherwise specified.

Amino Acid Numbering. CB2 residues mentioned in the text are referred to by using the amino acid numbering scheme of Ballesteros and Weinstein;[48] for example, K3.28(109). Number of the transmembrane helix (TM) follows the one-letter amino acid code, and the sequence number is at the end in the brackets. The digit in the middle reveals the relative location of the residue in regard with the most highly conserved (0.50) residue of the TM domain.

Comparative Model of CB2. We used the same procedure and methods to model the CB2 receptor as previously described for the CB1 receptor.[26] See Supporting Information for the multiple sequence alignment of the CB2 sequence with other homologous GPCR sequences (Section K), prediction of the TM residues with different secondary structure prediction methods[49−54] (Section L), and the final modeling alignment of the human CB2 sequence with the bovine rhodopsin template (PDB code 1hzx; Section C). Furthermore, Domain Fishing[55] server was used to provide additional assistance in the modeling alignment (Supporting Information, Section B).

Coordinates for the first and third extracellular loop (E1 and E3) were extracted directly from the rhodopsin template, while the InsightII loop search procedure was used for the generation of the other loops. The optimized receptor structure was subjected to a 500-ps constrained MD simulation in a TIP4P[56] water box as previously described for the CB1 model and the rhodopsin crystal structure[26] (see Supporting Information, Section M for the detailed MD parameters). Similarly to CB1, 100 different conformations of the CB2 model were created in a simulated annealing procedure to explore the positions of the protein side chains in the receptor binding site (see ref 26). The final frame (500 ps; model 1) from the MD run was used as the starting structure. Only the residues within a 20-Å-radius sphere surrounding the phenylalanine F3.36(117) were allowed to move during the process. Out of these 100 conformations, four distinct receptor conformers (models 2−5) were chosen for the subsequent analysis using the same SOM (self-organizing map)-based procedure as described for the CB1 model.[26]

Choice for the Receptor Conformer. Five different receptor conformers (models 1−5; see above) were used for docking 39 CB2 ligands at the putative binding site of the receptor (See Supporting Information, Section A for the structures of **1**−**39**). The ligands were automatically docked within an 18-Å distance from the backbone oxygen of lysine K3.28(109). Maximally 25 different conformations were produced for each ligand. All docking conformations were ranked according to the CScore consensus scoring value. To evaluate which receptor conformer would be the 'best' choice to utilize in the database searches, we built crude CoMFA[45] models using the best-ranked ligand conformations at each different receptor binding site. Gasteiger−Hückel charges[57,58] were applied on the ligand structures. Both electrostatic and steric interaction fields were calculated using the SYBYL default settings. Column filtering was set to 2.0 kcal/mol to improve the signal-noise ratio. Ligand binding affinities (pK_i) at CB2 were collected from literature[9,15,16,59−73] and used as dependent variables (Supporting Information, Section A). After an initial random group cross-validation (leave-10%-out) and removal of outliers, a recently introduced validation method, progressive scrambling[74,75] was applied on the resulting PLS models. Evaluation of r_{yy}^2 (correlation between the original and scrambled responses) was conducted at the critical threshold level of perturbation $s = 0.85$. These validation results guided the choice of the receptor conformer to be used in the database searches.

Database Searches. We built three different database queries utilizing the docked CB2 ligands and the structure of the receptor binding site. The first query (Q1) was based on six ligand structures in their docking positions; the potent nonselective cannabinoid agonists **7** and **16**, and the selective CB2 agonists **11**, **12**, **17**, and **26** (see Supporting Information, Section A for the structures). Structure of **7** was used to define the query features: oxygen atom of the C11 hydroxyl (northern aliphatic hydroxyl, NAH) as a H-bond acceptor site (tolerance 0.8 Å); C1 hydroxyl (phenolic hydroxyl) as a donor site (tolerance 1.0 Å), carbons C7 and C7′ as hydrophobic sites (tolerance 1.0 Å). The multiple volume surface of all six ligands was calculated and used as a surface volume constraint (tolerance 1.0 Å). Additionally, a partial match constraint was applied on the hydrophobic sites so that at least one of them had to match with the hit molecules. The second query (Q2) was created from the receptor binding cavity surrounding the docked molecules. The side chain nitrogen of K3.28(109) and the hydroxy oxygen of S2.60(90) were defined as H-bond donors and the hydroxy oxygen of T3.33(114) as an acceptor (tolerance 0.75 Å). A Connolly[76] surface was calculated for the receptor residues within a 3-Å shell around **7** and used as a surface volume constraint (tolerance 1.5 Å) to exclude the region occupied by the receptor. At least one acceptor/donor or maximally two such features were required from the hit molecules by using the partial match constraint. Features from both the receptor binding site and the docked ligands (**7**, **16**, and **17**) were combined in the third query (Q3). NAH oxygen of **16** (C1 hydroxyl) and **17** (C1 hydroxymethyl) as well as pyranyl oxygen of **7** were defined as acceptor atoms. The corresponding donor sites at the protein were S7.39(285) for **16** and S2.60(90) for **17**. The phenolic hydroxyl of **7** was defined as a donor atom and the backbone oxygen of K3.28(109) represented the corresponding acceptor site at the receptor. Also, the side chain nitrogen of K3.28(109) and the hydroxy oxygen of T3.33(114) were defined as H-bond donors. The tolerance of all the acceptor/donor features was set to 0.75 Å. A hydrophobic feature was placed near the last carbons of the ligand aliphatic side chain (tolerance 1.0 Å). A surface volume constraint (tolerance 1.5 Å) was created using a MOLCAD[77]-separated surface that was calculated between the three ligands and the receptor residues within a 3-Å shell around **7**. Moreover, partial match constraint was applied on all the ligand acceptor/donor atoms and the donor features of K3.28-(109) and T3.33(114); hit molecules had to match at least two and at most three of these features. Q1 and Q3 were used to search through the Maybridge database (April 2003) and Q2 was used to further filter the hits obtained with Q1 and Q3. In all searches, the query type was set to Flex Search, time limit to 10 s/molecule, and maximum molecular weight to 400 g/mol.

Filtering the Hit Molecules for Biological Evaluation. The hit molecules obtained with all queries were docked at the CB2 receptor (model 1) in the same way as previously described for the 39 CB2 ligands. Due to the great number of molecules, the program was allowed to produce only up to 10 conformations for each hit. The resulting docking conformations were ranked with CScore and the Q1 and Q3 hits also with X-Score. All molecules from the Q2 results that had a conformer with a CScore value of 4−5 were chosen for further analysis. From the Q1 and Q3 results, we chose the molecules which had a conformer with both good CScore and X-Score values: a CScore value of 3−5 and an X-Score rank position of 1−75 or 1−25, respectively. Finally, the chosen hits were visually checked by the synthetic chemists of our laboratory to decide which of them should be ordered and tested for biological activity at CB2.

Biological Evaluation of Hits. CB2 receptor-dependent G-protein activities of the hit molecules were determined using the [^{35}S]GTPγS binding assay. Ligand activities at the human CB2 receptor were first screened in lysates prepared from stably transfected CHO-hCB2 cells, and full dose−responses were determined in CHO-hCB2 cell membranes as previously described.[78] Active compounds were tested also in nontransfected CHO cells to confirm their CB2 receptor-dependent activity. Ligand activities at the CB1 receptor were tested in optimized [^{35}S]GTPγS binding conditions using rat cerebellar membranes as previously described.[79] Results are presented as mean ± SEM of at least three independent experiments performed in duplicate. Data-analysis was calculated as nonlinear regressions by GraphPad Prism 4.0.

Acknowledgment. This work was supported by ISB (The National Graduate School in Informational and Structural Biology), National Technology Agency of Finland, and Academy of Finland (grant #107300). CSC − Scientific Computing, Ltd. is gratefully acknowledged for computational resources. We also thank Toni Rönkkö (M.Sc.), Ms. Helly Rissanen, and Ms. Minna Glad for their technical assistance.

Supporting Information Available: These include, for example, multiple sequence alignment of the CB receptors and other related GPCRs, prediction of the CB2 TM helix residues, Domain Fishing results, modeling alignment of the human CB2 receptor and bovine rhodopsin sequence, MD parameters, PROCHECK summaries, ligand molecular structures and CB2 binding affinities used in the CoMFA models, and PLS and progressive scrambling statistics for the CB2 CoMFA models. This material is available free of charge via the Internet at http://pubs.acs.org.

References

(1) Munro, S.; Thomas, K. L.; Abu-Shaar, M. Molecular characterization of a peripheral receptor for cannabinoids. *Nature* **1993**, *365*, 61−65.

(2) Galiegue, S.; Mary, S.; Marchand, J.; Dussossoy, D.; Carriere, D.; Carayon, P.; Bouaboula, M.; Shire, D.; Le Fur, G.; Casellas, P. Expression of central and peripheral cannabinoid receptors in human immune tissues and leukocyte subpopulations. *Eur. J. Biochem.* **1995**, *232*, 54−61.

(3) Di Marzo, V.; Bifulco, M.; De Petrocellis, L. The endocannabinoid system and its therapeutic exploitation. *Nat. Rev. Drug Discovery* **2004**, *3*, 771−784.

(4) Cravatt, B. F.; Lichtman, A. H. The endogenous cannabinoid system and its role in nociceptive behavior. *J. Neurobiol.* **2004**, *61*, 149−160.

(5) Piomelli, D. The endogenous cannabinoid system and the treatment of marijuana dependence. *Neuropharmacology* **2004**, *47* Suppl 1, 359−367.

(6) Rodriguez de Fonseca, F.; Del Arco, I.; Bermudez-Silva, F. J.; Bilbao, A.; Cippitelli, A.; Navarro, M. The endocannabinoid system: physiology and pharmacology. *Alcohol Alcohol.* **2005**, *40*, 2−14.

(7) Goutopoulos, A.; Makriyannis, A. From cannabis to cannabinergics: new therapeutic opportunities. *Pharmacol. Ther.* **2002**, *95*, 103−117.

(8) Malan, T. P., Jr.; Ibrahim, M. M.; Lai, J.; Vanderah, T. W.; Makriyannis, A.; Porreca, F. CB2 cannabinoid receptor agonists: pain relief without psychoactive effects? *Curr. Opin. Pharmacol.* **2003**, *3*, 62−67.

(9) Iwamura, H.; Suzuki, H.; Ueda, Y.; Kaya, T.; Inaba, T. In vitro and in vivo pharmacological characterization of JTE−907, a novel selective ligand for cannabinoid CB2 receptor. *J. Pharmacol. Exp. Ther.* **2001**, *296*, 420−425.

(10) Patel, H. J.; Birrell, M. A.; Crispino, N.; Hele, D. J.; Venkatesan, P.; Barnes, P. J.; Yacoub, M. H.; Belvisi, M. G. Inhibition of guinea-pig and human sensory nerve activity and the cough reflex in guinea-pigs by cannabinoid (CB2) receptor activation. *Br. J. Pharmacol.* **2003**, *140*, 261−268.

(11) Sanchez, C.; de Ceballos, M. L.; del Pulgar, T. G.; Rueda, D.; Corbacho, C.; Velasco, G.; Galve-Roperh, I.; Huffman, J. W.; Ramon y Cajal, S.; Guzman, M. Inhibition of glioma growth in vivo by selective activation of the CB(2) cannabinoid receptor. *Cancer Res.* **2001**, *61*, 5784−5789.

(12) McKallip, R. J.; Lombard, C.; Fisher, M.; Martin, B. R.; Ryu, S.; Grant, S.; Nagarkatti, P. S.; Nagarkatti, M. Targeting CB2 cannabinoid receptors as a novel therapy to treat malignant lymphoblastic disease. *Blood* **2002**, *100*, 627−634.

(13) Bab, I.; Ofek, O.; Karsak, M.; Fogel, M.; Wright, K.; Attar-Namdar, M.; Shohami, E.; Zimmer, A.; Mechoulam, R. Cannabinoid CB2 receptor and human osteoporosis. *2004 Symposium on the Cannabinoids*; International Cannabinoid Research Society: Burlington, VT, 2004; p 74.

(14) Gaoni, Y.; Mechoulam, R. Isolation, Structure, and Partial Synthesis of an Active Constituent of Hashish. *J. Am. Chem. Soc.* **1964**, *86*, 1646−1647.

(15) Huffman, J. W.; Liddle, J.; Yu, S.; Aung, M. M.; Abood, M. E.; Wiley, J. L.; Martin, B. R. 3-(1′,1′-Dimethylbutyl)-1-deoxy-delta8-THC and related compounds: synthesis of selective ligands for the CB2 receptor. *Bioorg. Med. Chem.* **1999**, *7*, 2905−2914.

(16) Hanus, L.; Breuer, A.; Tchilibon, S.; Shiloah, S.; Goldenberg, D.; Horowitz, M.; Pertwee, R. G.; Ross, R. A.; Mechoulam, R.; Fride, E. HU-308: a specific agonist for CB(2), a peripheral cannabinoid receptor. *Proc. Natl. Acad. Sci. U.S.A.* **1999**, *96*, 14228−14233.

(17) Malan, T. P., Jr.; Ibrahim, M. M.; Deng, H.; Liu, Q.; Mata, H. P.; Vanderah, T.; Porreca, F.; Makriyannis, A. CB2 cannabinoid receptor-mediated peripheral antinociception. *Pain* **2001**, *93*, 239−245.

(18) Valenzano, K. J.; Tafesse, L.; Lee, G.; Harrison, J. E.; Boulet, J. M.; Gottshall, S. L.; Mark, L.; Pearson, M. S.; Miller, W.; Shan, S.; Rabadi, L.; Rotshteyn, Y.; Chaffer, S. M.; Turchin, P. I.; Elsemore, D. A.; Toth, M.; Koetzner, L.; Whiteside, G. T. Pharmacological and pharmacokinetic characterization of the cannabinoid receptor 2 agonist, GW405833, utilizing rodent models of acute and chronic pain, anxiety, ataxia and catalepsy. *Neuropharmacology* **2005**, *48*, 658−672.

(19) Rinaldi-Carmona, M.; Barth, F.; Millan, J.; Derocq, J. M.; Casellas, P.; Congy, C.; Oustric, D.; Sarran, M.; Bouaboula, M.; Calandra, B.; Portier, M.; Shire, D.; Breliere, J. C.; Le Fur, G. L. SR 144528, the first potent and selective antagonist of the CB2 cannabinoid receptor. *J. Pharmacol. Exp. Ther.* **1998**, *284*, 644−650.

(20) Palczewski, K.; Kumasaka, T.; Hori, T.; Behnke, C. A.; Motoshima, H.; Fox, B. A.; Le Trong, I.; Teller, D. C.; Okada, T.; Stenkamp, R. E.; Yamamoto, M.; Miyano, M. Crystal structure of rhodopsin: A G protein-coupled receptor. *Science* **2000**, *289*, 739−745.

(21) Bissantz, C.; Bernard, P.; Hibert, M.; Rognan, D. Protein-based virtual screening of chemical databases. II. Are homology models of G-protein coupled receptors suitable targets? *Proteins* **2003**, *50*, 5−25.

(22) Evers, A.; Klabunde, T. Structure-based drug discovery using GPCR homology modeling: successful virtual screening for antagonists of the alpha1A adrenergic receptor. *J. Med. Chem.* **2005**, *48*, 1088−1097.

(23) Varady, J.; Wu, X.; Fang, X.; Min, J.; Hu, Z.; Levant, B.; Wang, S. Molecular modeling of the three-dimensional structure of dopamine 3 (D3) subtype receptor: discovery of novel and potent D3 ligands through a hybrid pharmacophore- and structure-based database searching approach. *J. Med. Chem.* **2003**, *46*, 4377−4392.

(24) Xie, X. Q.; Chen, J. Z.; Billings, E. M. 3D structural model of the G-protein-coupled cannabinoid CB2 receptor. *Proteins* **2003**, *53*, 307−319.

(25) Montero, C.; Campillo, N. E.; Goya, P.; Paez, J. A. Homology models of the cannabinoid CB1 and CB2 receptors. A docking analysis study. *Eur. J. Med. Chem.* **2005**, *40*, 75−83.

(26) Salo, O. M.; Lahtela-Kakkonen, M.; Gynther, J.; Jarvinen, T.; Poso, A. Development of a 3D model for the human cannabinoid CB1 receptor. *J. Med. Chem.* **2004**, *47*, 3048−3057.

(27) Zhang, R.; Hurst, D. P.; Barnett-Norris, J.; Reggio, P. H.; Song, Z. H. Cysteine 2.59(89) in the second transmembrane domain of human CB2 receptor is accessible within the ligand binding crevice: evidence for possible CB2 deviation from a rhodopsin template. *Mol. Pharmacol.* **2005**, *68*, 69−83.

(28) Tao, Q.; McAllister, S. D.; Andreassi, J.; Nowell, K. W.; Cabral, G. A.; Hurst, D. P.; Bachtel, K.; Ekman, M. C.; Reggio, P. H.; Abood, M. E. Role of a conserved lysine residue in the peripheral cannabinoid receptor (CB2): evidence for subtype specificity. *Mol. Pharmacol.* **1999**, *55*, 605−613.

(29) Rhee, M. H. Functional role of serine residues of transmembrane dopamin VII in signal transduction of CB2 cannabinoid receptor. *J. Vet. Sci.* **2002**, *3*, 185−191.

(30) McAllister, S. D.; Rizvi, G.; Anavi-Goffer, S.; Hurst, D. P.; Barnett-Norris, J.; Lynch, D. L.; Reggio, P. H.; Abood, M. E. An aromatic microdomain at the cannabinoid CB(1) receptor constitutes an agonist/inverse agonist binding region. *J. Med. Chem.* **2003**, *46*, 5139−5152.

(31) Rhee, M. H.; Nevo, I.; Bayewitch, M. L.; Zagoory, O.; Vogel, Z. Functional role of tryptophan residues in the fourth transmembrane domain of the CB(2) cannabinoid receptor. *J. Neurochem.* **2000**, *75*, 2485−2491.

(32) McAllister, S. D.; Tao, Q.; Barnett-Norris, J.; Buehner, K.; Hurst, D. P.; Guarnieri, F.; Reggio, P. H.; Nowell Harmon, K. W.; Cabral, G. A.; Abood, M. E. A critical role for a tyrosine residue in the cannabinoid receptors for ligand recognition. *Biochem. Pharmacol.* **2002**, *63*, 2121−2136.

(33) McAllister, S. D.; Hurst, D. P.; Barnett-Norris, J.; Lynch, D.; Reggio, P. H.; Abood, M. E. Structural mimicry in class A G protein-coupled receptor rotamer toggle switches: the importance of the F3.36(201)/W6.48(357) interaction in cannabinoid CB1 receptor activation. *J. Biol. Chem.* **2004**, *279*, 48024−48037.

(34) Singh, R.; Hurst, D. P.; Barnett-Norris, J.; Lynch, D. L.; Guarnieri, F.; Reggio, P. H. Activation of the cannabinoid CBI receptor involves a W6.48/F3.36 rotamer toggle switch. *Biophys. J.* **2003**, *84*, 497a−497a.

(35) Saario, S. M.; Savinainen, J. R.; Laitinen, J. T.; Jarvinen, T.; Niemi, R. Monoglyceride lipase-like enzymatic activity is responsible for hydrolysis of 2-arachidonoylglycerol in rat cerebellar membranes. *Biochem. Pharmacol.* **2004**, *67*, 1381−1387.

(36) *InsightII v. 2000*; Accelrys, Inc.: San Diego, CA. http://www.accelrys.com/.

(37) *SYBYL v. 6.9*, Tripos Associates, Inc.: St. Louis, MO. http://www.tripos.com/.

(38) *GROMACS, v. 3.1.4*; Department of Biophysical Chemistry, University of Groningen. Nijenborgh 4, 9747 AG Groningen, The Netherlands. http://www.gromacs.org/.

(39) Lindahl, E.; Hess, B.; van der Spoel, D. GROMACS 3.0: A package for molecular simulation and trajectory analysis. *J. Mol. Mod.* **2001**, *7*, 306−317.

(40) Laskowski, R. A.; MacArthur, M. W.; Moss, D. S.; Thornton, J. M. PROCHECK: a program to check the stereochemical quality of protein structures. *J. Appl. Crystallogr.* **1993**, *26*, 283−291. http://www.biochem.ucl.ac.uk/~roman/procheck/procheck.html.

(41) *GOLD v. 2.0*; Cambridge Crystallographic Data Centre: Cambridge, U.K. http://www.ccdc.cam.ac.uk/products/life_sciences/gold/.

(42) CScore. Tripos Associates, Inc.: St. Louis, MO. http://www.tripos.com/sciTech/inSilicoDisc/virtualScreening/cscore.html#references.

(43) Wang, R.; Lai, L.; Wang, S. Further Development and Validation of Empirical Scoring Functions for Structure-Based Binding Affinity Prediction. *J. Comput.-Aided Mol. Des.* **2002**, *16*, 11−26.

(44) Wang, R.; Lu, Y.; Wang, S. Comparative evaluation of 11 scoring functions for molecular docking. *J. Med. Chem.* **2003**, *46*, 2287−2303.
(45) Cramer, R. D., III; Patterson, D. E.; Bunce, J. D. Comparative Molecular Field Analysis (CoMFA). 1. Effect of Shape on Binding of Steroids to Carrier Proteins. *J. Am. Chem. Soc.* **1988**, *110*, 5959−5967.
(46) *Maybridge Database*, April2003; Maybridge Chemical Company Ltd: Trevillett, Tintagel, Cornwall PL34 OHW, England. http://www.maybridge.com/.
(47) *UNITY*. Tripos Associates, Inc.: St. Louis, MO. http://www.tripos.com/sciTech/inSilicoDisc/chemInfo/unity.html.
(48) Ballesteros, J. A.; Weinstein, H. W. Integrated methods for the construction of three-dimensional models and computational probing of structure−function relations in G-protein coupled receptors. In *Methods in Neuroscience*; Conn, P. M., Sealfon, S. C., Eds.; Academic Press: San Diego, 1995; Vol. 25, pp 366−428.
(49) Hofmann, K.; Stoffel, W. TMbase − A database of membrane spanning proteins segments; http://www.ch.embnet.org/software/TMPRED_form.html. *Biol. Chem. Hoppe-Seyler* **1993**, *374*, 166.
(50) Jones, D. T. Protein secondary structure prediction based on position-specific scoring matrices. *J. Mol. Biol.* **1999**, *292*, 195−202.
(51) Juretic, D.; Zoranic, L.; Zucic, D. Basic charge clusters and predictions of membrane protein topology. *J. Chem. Inf. Comput. Sci.* **2002**, *42*, 620−632.
(52) Rost, B. PHD: predicting one-dimensional protein structure by profile-based neural networks. *Methods Enzymol.* **1996**, *266*, 525−539.
(53) Tusnady, G. E.; Simon, I. The HMMTOP transmembrane topology prediction server. *Bioinformatics* **2001**, *17*, 849−850. http://www.enzim.hu/hmmtop/.
(54) von Heijne, G. Membrane Protein Structure Prediction: Hydrophobicity Analysis and the 'Positive Inside' Rule. *J. Mol. Biol.* **1992**, *225*, 487−494.
(55) Contreras-Moreira, B.; Bates, P. A. Domain Fishing: a first step in protein comparative modelling. *Bioinformatics* **2002**, *18*, 1141−1142.
(56) Jorgensen, W. L.; Chandrasekhar, J.; Madura, J. D.; Impey, R. W.; Klein, M. L. Comparison of simple potential functions for simulating liquid water. *J. Chem. Phys.* **1983**, *79*, 926−935.
(57) Gasteiger, J.; Marsili, M. Iterative partial equalization of orbital electronegativity: a rapid access to atomic charges. *Tetrahedron* **1980**, *36*, 3219−3222.
(58) Purcell, W. P.; Singer, J. A. A Brief Review and Table of Semiempirical Parameters Used in the Hückel Molecular Orbital Method. *J. Chem. Eng. Data* **1967**, *12*, 235−246.
(59) Aung, M. M.; Griffin, G.; Huffman, J. W.; Wu, M.; Keel, C.; Yang, B.; Showalter, V. M.; Abood, M. E.; Martin, B. R. Influence of the N-1 alkyl chain length of cannabimimetic indoles upon CB-(1) and CB(2) receptor binding. *Drug Alcohol Depend.* **2000**, *60*, 133−140.
(60) Ben-Shabat, S.; Fride, E.; Sheskin, T.; Tamiri, T.; Rhee, M. H.; Vogel, Z.; Bisogno, T.; De Petrocellis, L.; Di Marzo, V.; Mechoulam, R. An entourage effect: inactive endogenous fatty acid glycerol esters enhance 2-arachidonoyl-glycerol cannabinoid activity. *Eur. J. Pharmacol.* **1998**, *353*, 23−31.
(61) Cheng, Y.-X.; Tomaszewski, M.; Walpole, C.; Yang, H. Novel alkoxyarylbenzimidazoles as CB2 receptor agonists. WO Patent 02/085866, 2002.
(62) Gallant, M.; Dufresne, C.; Gareau, Y.; Guay, D.; Leblanc, Y.; Prasit, P.; Rochette, C.; Sawyer, N.; Slipetz, D. M.; Tremblay, N.; Metters, K. M.; Labelle, M. New class of potent ligands for the human peripheral cannabinoid receptor. *Bioorg. Med. Chem. Lett.* **1996**, *6*, 2263−2268.
(63) Hanasaki, K.; Murashi, T.; Kai, H. 2-Imino-1,3-thiazine derivatives. WO Patent 01/19807, 2001.
(64) Huffman, J. W.; Yu, S.; Showalter, V.; Abood, M. E.; Wiley, J. L.; Compton, D. R.; Martin, B. R.; Bramblett, R. D.; Reggio, P. H. Synthesis and pharmacology of a very potent cannabinoid lacking a phenolic hydroxyl with high affinity for the CB2 receptor. *J. Med. Chem.* **1996**, *39*, 3875−3877.
(65) Ibrahim, M. M.; Deng, H.; Zvonok, A.; Cockayne, D. A.; Kwan, J.; Mata, H. P.; Vanderah, T. W.; Lai, J.; Porreca, F.; Makriyannis, A.; Malan, T. P., Jr. Activation of CB2 cannabinoid receptors by AM1241 inhibits experimental neuropathic pain: pain inhibition by receptors not present in the CNS. *Proc. Natl. Acad. Sci. U.S.A.* **2003**, *100*, 10529−10533.
(66) Inaba, T.; Kaya, T.; Iwamura, H. Novel compounds and pharmaceutical use thereof. WO Patent 97/29079, 1997.
(67) Inaba, T.; Kaya, T.; Iwamura, H. 2-oxoquinoline compounds and medicinal uses thereof. WO Patent 00/40562, 2000.
(68) Inaba, T.; Kaya, T.; Iwamura, H. Quinoline compounds and medicinal uses thereof. WO Patent 99/02499, 1999.
(69) Kai, H.; Murashi, T.; Tomida, M. Medicinal composition containing 1,3-thiazine derivative. WO Patent 02/072562, 2002.
(70) Lin, S.; Khanolkar, A. D.; Fan, P.; Goutopoulos, A.; Qin, C.; Papahadjis, D.; Makriyannis, A. Novel analogues of arachidonylethanolamide (anandamide): affinities for the CB1 and CB2 cannabinoid receptors and metabolic stability. *J. Med. Chem.* **1998**, *41*, 5353−5361.
(71) Makriyannis, A.; Khanolkar, A. Novel bicyclic cannabinoid agonists for the cannabinoid receptor. WO Patent 01/028497, 2001.
(72) Ross, R. A.; Brockie, H. C.; Stevenson, L. A.; Murphy, V. L.; Templeton, F.; Makriyannis, A.; Pertwee, R. G. Agonist-inverse agonist characterization at CB1 and CB2 cannabinoid receptors of L759633, L759656, and AM630. *Br. J. Pharmacol.* **1999**, *126*, 665−672.
(73) Showalter, V. M.; Compton, D. R.; Martin, B. R.; Abood, M. E. Evaluation of binding in a transfected cell line expressing a peripheral cannabinoid receptor (CB2): identification of cannabinoid receptor subtype selective ligands. *J. Pharmacol. Exp. Ther.* **1996**, *278*, 989−999.
(74) Clark, R. D.; Sprous, D. G.; Leonard, J. M. Validating models based on large data sets. In *Rational Approaches to Drug Design*; Sippl, W., Ed.; Prous Science: Barcelona, 2001; pp 475−485.
(75) Clark, R. D.; Fox, P. C. Statistical variation in progressive scrambling. *J. Comput.-Aided Mol. Des.* **2004**, *17*, 1−14.
(76) Connolly, M. L. Solvent-accessible surfaces of proteins and nucleic acids. *Science* **1983**, *221*, 709−713.
(77) Brickmann, J.; Goetze, T.; Heiden, W.; Moeckel, G.; Reiling, S.; Vollhardt, H.; Zachmann, C.-D. Interactive Visualization of Molecular Scenarios with MOLCAD/SYBYL. In: Data Visualization in Molecular Science − Tools for Insight and Innovation; Bowie, J. E., Ed.; Addison-Wesley Publishing Company Inc.: Reading, MA, 1995; pp 83−97. http://ws05.pc.chemie.tu-darmstadt.de/research/molcad/Molcad_sub_index.html. http://www.tripos.com/data/SYBYL/Molcad_072505.pdf.
(78) Savinainen, J. R.; Kokkola, T.; Salo, O. M.; Poso, A.; Jarvinen, T.; Laitinen, J. T. Identification of WIN55212−3 as a competitive neutral antagonist of the human cannabinoid CB(2) receptor. *Br. J. Pharmacol.* **2005**, *145*, 636−645.
(79) Savinainen, J. R.; Saario, S. M.; Niemi, R.; Jarvinen, T.; Laitinen, J. T. An optimized approach to study endocannabinoid signaling: evidence against constitutive activity of rat brain adenosine A1 and cannabinoid CB1 receptors. *Br. J. Pharmacol.* **2003**, *140*, 1451−1459.

JM050565B